# Effect of oxygen vacancies on the electronic and optical properties of vanadium dioxide

J.-R. LIANG[*], M.-J. WU, N. LI, X. LIU
*School of Electronic Information Engineering, Tianjin University, Tianjin 300072, P. R. China*

We calculated the electronic structure and optical properties of monoclinic vanadium dioxide ($VO_2$) containing different amount of oxygen vacancies in the scheme of GGA+$U$. The O-vacancy concentrations were set as 0%, 1.04% and 2.08%, respectively. Our results show that the band gap descends as the O-vacancy concentration ascends in $VO_2$ (M1), indicating that O vacancies contribute to the process of metal-insulator transition (MIT) in $VO_2$ by reducing the energy barrier needed for phase transition. Besides, O vacancies also affect the optical transition properties of $VO_2$. As the number of O vacancies increases in $VO_2$ (M1), the light transmittance decreases in the infrared range and increases in the visible and ultraviolet region, which has rarely been studied in theoretical simulation works. Studying the effect of O vacancies on the phase transition properties of $VO_2$ may help to understand its phase change mechanism and extend its application.

## 1. Introduction

Vanadium dioxide ($VO_2$), a prototype of strongly correlated materials, undergoes a first-order transition from a low temperature insulating phase to a high temperature metallic phase near room temperature (341 K) with a structural transformation from the monoclinic (M1 phase) to the rutile tetragonal structure (R phase) [1]. In the meantime, a significant change of optical transmittance and reflectance also occurs [2-5].

Despite the wide applications of $VO_2$, the mechanism driving the MIT is still debated since both the electron correlation and lattice distortion effects are proved to trigger the phase transition [6,7]. Recently, the oxygen vacancy is found to play an important role in the metal-insulator transition properties of vanadium dioxide. Kannatassen Appavoo *et al.* studied the oxygen vacancies at grain boundaries of $VO_2$ nanoparticles and found that oxygen vacancies can act as nucleation sites that lower the energy required to effect the transition [8]. Lele Fan *et al.* reported that oxygen vacancies in $VO_2$ can trigger an earlier onset of the metal states. Both of them found the importance of oxygen vacancies in the $VO_2$ materials [9]. However, their research mainly focused on the experimental aspects and the theoretical study of O vacancies is deficient. We studied the more general case of crystal $VO_2$ by the approach of generalized gradient approximation plus $U$ (GGA+$U$) based on density functional theory (DFT) and our calculations are consistent with the experimental results. As we all know, insulating $VO_2$ is one of the correlated materials that have attracted tremendous interest and have been widely studied.

Jaewoo Jeong *et al.* showed the electrolyte gating of $VO_2$ leads to the metallization of the insulating phase under phase transition temperature, which is related to the electric field-induced creation of oxygen vacancies [10]. Julie Karel *et al.* found that the electronic structures of thermally induced and the gate-induced metallic phases in $VO_2$ thin films were different, which indicates the distinct mechanisms of their origins and the latter is also consistent with the formation of oxygen vacancies from electrolyte gating [11]. Thus, studies on oxygen vacancies may probably be helpful for understanding the underlying physical mechanism of MIT in $VO_2$. However, few theoretical works of the effect of oxygen vacancies on the optical properties have been reported and our research will shed some light on the role of oxygen vacancies in the phase transition of $VO_2$.

Our previous experimental study has shown that both the phase transition temperature and the hysteresis width decreases as the $VO_2$ film thickness increases, owing to the higher concentration carriers resulted from the oxygen vacancies of uncompleted lattice in $VO_2$ thin films [12]. In this work, we calculated the electronic structure, electron density difference and optical properties of $VO_2$(M1) supercells containing different concentrations of oxygen vacancies to study the effect of O vacancies on both electronic and optical properties of $VO_2$.

## 2. Calculation methods

The crystal structures of $VO_2$ used are taken from experiments. The insulating M1 phase has a monoclinic

space group of $P2_1/c$ and lattice parameters are $a$ = 5.743 Å, $b$ = 4.517 Å, $c$ = 5.375 Å, $\beta$ = 122.61° and $Z$ = 4 [13], the unit cell of which is twice as large as the tetragonal structure. The atomic positions in the monoclinic structure are V = (0.242, 0.975, 0.025), O1 = (0.100, 0.210, 0.200) and O2 = (0.390, 0.690, 0.290). Calculations are implemented in the CASTEP code and based on density functional theory (DFT) within plane wave pseudopotentials and generalized gradient approximation (GGA) in the scheme of Perdew-Burke-Ernzerhof (PBE) exchange-correlation functional.

Since the calculations based on local density (LDA) or generalized gradient approximation (GGA) failed to reproduce a finite band gap in the M1 phase [14,15], an GGA+$U$ ($U$ is the Coulomb repulsion parameter) approach was utilized in the calculations. The on-site Coulomb correction applied to the $3d$ orbital electrons of V was taken as $U$ = 5.0 eV and calculations were performed on a $2 \times 2 \times 2$ VO$_2$ supercell with 96 atoms. The electron function was expanded in terms of plane-wave basis set with a cutoff energy of 340 eV and a Monkhorst-Pack k-point mesh of $1 \times 1 \times 1$ was used for geometry optimization and property calculations. The convergence criterion of energy tolerance was $2.0 \times 10^{-5}$ eV/atom. The maximal force, stress and displacement were 0.05 eV/Å, 0.1 GPa and $2.0 \times 10^{-3}$ Å.

## 3. Results and discussion

### 3.1 Atomic structure and electron density difference

The atomic structures of supercells of M1-phase vanadium dioxide containing different oxygen-vacancy concentrations are shown in Fig.1. The dimerization between V atoms along the rutile c axis can be seen clearly, which is the symbol of insulating phase of VO$_2$. Here, Fig. 1(a), (b) and (c) show the 96-atom pristine VO$_2$ supercell ($V_{32}O_{64}$), the 95-atom supercell with one O vacancy ($V_{32}O_{63}$) and the 94-atom supercell with two O vacancies ($V_{32}O_{62}$), respectively. The large grey spheres represent vanadium atoms and the small red spheres are oxygen atoms. The vacancies are marked with black stars.

In order to better understand the change of the electronic structure, the electron density difference is calculated and we can see the charge flow around O vacancies intuitively in Fig. 1(d), (e) and (f). The red and blue areas correspond to charge accumulation and depletion, respectively. Besides, oxygen vacancies not only change the electronic structure of VO$_2$ but also modify the atomic structure. When two O atoms were removed, the modification of charge density distribution extends to even farther areas in the supercell of monoclinic VO$_2$. Although the atomic structure around the O vacancies exhibit a little distortion, the V-V dimerization has been retained.
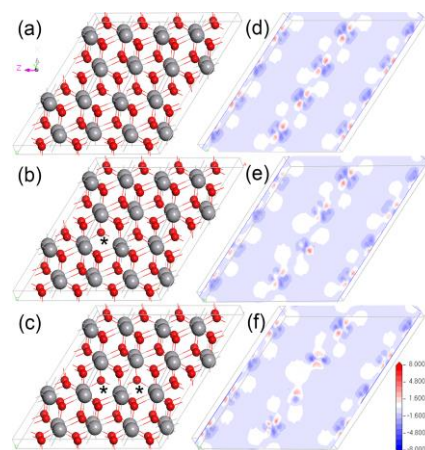


*Fig. 1. Atomic structure and electron density difference of supercells of (a)(d) pure M1-phase VO$_2$ ($V_{32}O_{64}$), (b)(e) with one oxygen vacancy ($V_{32}O_{63}$) and (c)(f) two oxygen vacancies ($V_{32}O_{62}$).*

### 3.2 Electronic properties

We calculated the electronic structures in the three situations. The band structures of pristine VO$_2$ (M1) and for the case of one O vacancy and two O vacancies were calculated with GGA+$U$. As is shown in Fig. 2, the band gaps of the three structures are 0.796 eV, 0.772 eV and 0.687 eV. The Fermi energy ($E_F$) is set as the energy level of the highest occupied state at 0 eV. The calculated bandgap of about 0.7 eV in monoclinic VO$_2$ is in agreement with the experimental results [16]. With the oxygen vacancies increasing in VO$_2$ (M1), the band gap becomes narrower. We also studied the supercells with different position of O vacancies. Even though the bandgap varies slightly, the decreasing trend with the increasing O vacancies has been the same. New states were introduced near the valence band maximum and the conduction band minimum when oxygen vacancies occur in VO$_2$ (M1), which agrees with the recent calculations [17].
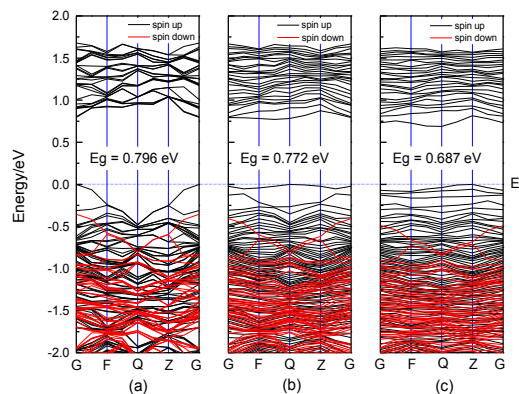


*Fig. 2. Band structure of supercell of (a) pure VO$_2$ (M1), (b) supercells with one oxygen vacancy and (c) two oxygen vacancies*

According to the results, the oxygen vacancies play an important role in the phase transition of $VO_2$ and decrease the energy barrier needed for the insulating phase transform to the metallic phase of $VO_2$ by reducing the band gap of $VO_2$ (M1). This agrees well with the recent experimental results [9,18]. This explains our previous results that the O vacancies of uncompleted lattice make the transition temperature lower and the hysteretic width narrower. Notably, as the V-V dimerization remained in the structure, it is probably the valence electrons introduced by removed O atoms to be the key factor making the band gap of $VO_2$ (M1) narrower.

Next, we calculated the total and partial density of states (DOS) of monoclinic $VO_2$. The results are shown in Fig. 3. The DOS near Fermi level is composed of V-3d and O-2p band from -8.1 to 0 4.6 eV. The valence band maximum (VBM) is mainly occupied by V-3d and O-2p electron states and their hybridization contributes to the formation of VBM. The conduction band minimum (CBM) is mainly occupied by V-3d electrons and they hybridizes with a small number of O-2p electrons.
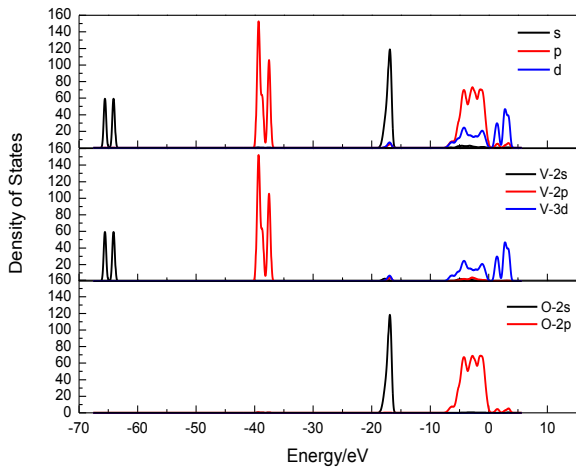


*Fig. 3. Total and partial density of states (DOS) of 96-atom supercell of pure monoclinic $VO_2$*

To compare the three conditions, the total density of states (TDOS) and partial density of states (PDOS) of pristine $VO_2$ (M1) supercell, supercells with one O vacancy and two O vacancies near the Fermi level are depicted in Fig. 4. The shift of curves in TDOS corresponding to the downshift of the band structure (see Fig. 2). The PDOS for V 3d states exhibited remarkable reduction of energy gap while the PDOS for O 2p states showed little change in the vicinity of Fermi level, indicating that the modification of V 3d states is the crucial factor causing the reduction of energy gap of TDOS in $VO_2$.
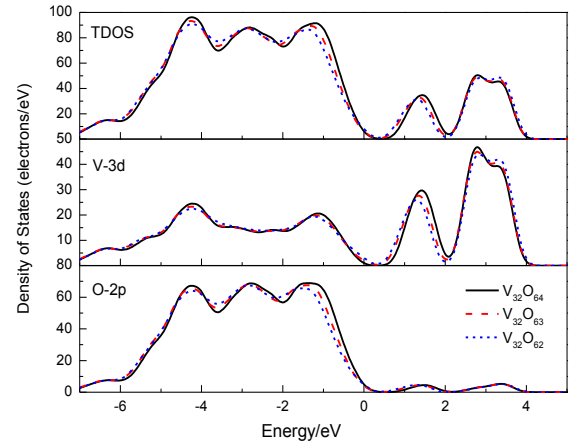


*Fig. 4. Total and partial DOS of pure $VO_2$ supercell ($V_{32}O_{64}$), supercells with one oxygen vacancy ($V_{32}O_{63}$) and two oxygen vacancies ($V_{32}O_{62}$)*

### 3.3 Optical properties

The effect of oxygen vacancies on the optical properties in $VO_2$ (M1) is also studied. As we all know, the complex dielectric function $\varepsilon(\omega) = \varepsilon_1(\omega) + i\varepsilon_2(\omega)$ can describe the optical properties of materials. Fig. 5(a) shows the real part ($\varepsilon_1(\omega)$) and imaginary part ($\varepsilon_2(\omega)$) of the dielectric function of monoclinic $VO_2$. The real part ($n$) and imaginary part ($k$) of refractive index are shown in Fig. 5(b). The peaks of both dielectric function and refractive index in the structures with O vacancies declined as compared with that of the pristine $VO_2$ structure. In Fig. 5(c), the absorption increases with the oxygen vacancy concentration with the photon energy ranging from about 0 eV to 1.59 eV, which corresponds to the infrared spectral range. The reflectivity also ascends with the O-vacancy concentration from about 0 eV to 0.87 eV and change slightly from 0.87 eV to 1.59 eV in Fig. 5(d), indicating that the reflectivity exhibit a similar tendency with the absorption. While in the visible and region (from about 1.59 eV to 6.20 eV), both of them present a general trend to decrease with the O-vacancy concentration. It is known that the sum of reflectivity, absorption and transmissivity of light in a material generally equals to one. Thus, we can deduce that the transmittance shows a contrary trend. In the infrared range, as the oxygen vacancy increases, the transmittance decreases while in the visible and ultraviolet region, it increases. Therefore, oxygen vacancies in $VO_2$ (M1) can reduce the transmission of light in the infrared range, which probably due to the increasing carrier concentration caused by the oxygen vacancies.

Because the phase transition temperature of $VO_2$ is near (a bit higher than) room temperature and the optical properties change remarkably, $VO_2$ becomes the promising material for optical switches, smart windows and so on [19-21]. On the one hand, as oxygen vacancies can reduce the phase transition energy and thus, reduce the phase transition temperature [18], introducing oxygen vacancies in $VO_2$ is an effective way to lower the transition temperature to the room temperature. On the other hand, reducing the transmittance of $VO_2$ (M1) with O vacancies

in the infrared range hinders the switching properties of light transmittance between the insulating phase and metallic phase.
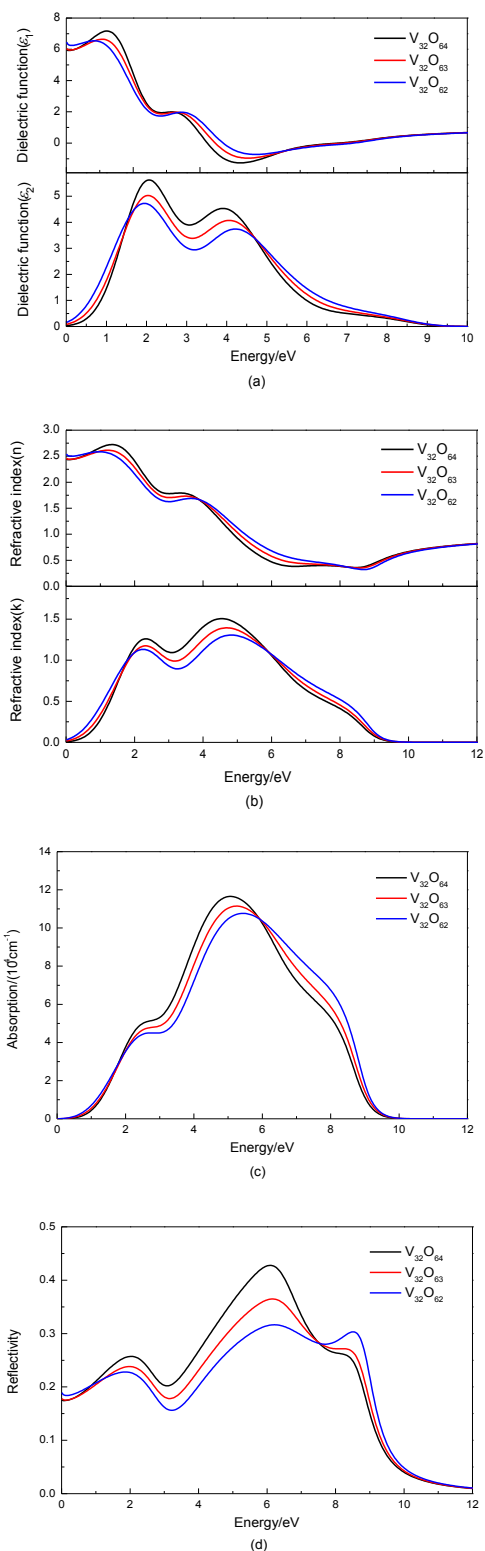


*Fig. 5. (a) Dielectric function, (b) refractive index, (c) absorption and (d) reflectivity of pure VO$_2$ (V$_{32}$O$_{64}$), with one oxygen vacancy (V$_{32}$O$_{63}$) and two oxygen vacancies (V$_{32}$O$_{62}$).*

## 4. Conclusion

The supercell of pure monoclinic VO$_2$ (M1), supercells containing one oxygen vacancy and two oxygen vacancies were calculated by the approach of GGA+$U$ based on density functional theory (DFT). The oxygen vacancy concentrations are about 0%, 1.04% and 2.08%, respectively. Our results show that the band gap descends as the O-vacancy concentration ascends in the M1-phase VO$_2$, reducing the energy barrier required for insulating VO$_2$ to transform to the metallic phase. The higher concentration of O vacancies lead to the destabilization of the insulating phase of VO$_2$. Considering the V-V dimerization has been retained, the introduction of valence electrons of removed O atoms is the key factor to reduce the band gap of insulating VO$_2$. Comparing the curves of TDOS and PDOS, the change of V 3d states is critical to the reduction of energy gap of VO$_2$. In terms of the optical properties, as the number of oxygen vacancies increases, the transmittance decreases in the infrared region and increases in the visible and ultraviolet region. Theoretical calculations may accelerate the research on optical properties of VO$_2$.

### References

[1] F. J. Morin, Phys. Rev. Lett. **3**, 34 (1959).
[2] R. Balu, P. V. Ashrit, Appl. Phys. Lett. **92**, 021904 (2008).
[3] F. Guinneton, L. Sauques, J. C. Valmalette, F. Cros, J. R. Gavarri, J. Phys. Chem. Solids. **62**, 1229 (2001).
[4] X. J. Wang, Y. Y. Liu, D. H. Li, B. H. Feng, Z. W. He, Z. Qi, Chin. Phys. B, **22**, 066803 (2013).
[5] H. Q. Zhu, Y. Li, G. X. Tong, B. Y. Fang, X. H. Wang, Optoelectron. Adv. Mat. **7**, 1015 (2013).
[6] R. Eguchi, M. Taguchi, M. Matsunami, K. Horiba, K. Yamamoto, Y. Ishida, A. Chainani, Y. Takata, M. Yabashi, D. Miwa, Y. Nishino, K. Tamasaku, T. Ishikawa, Y. Senba, H. Ohashi, Y. Muraoka, Z. Hiroi, S. Shin, Phys. Rev. B, **78**, 075115 (2008).
[7] S. Suga, A. Sekiyama, S. Imada, T. Miyamachi, H. Fujiwara, A. Yamasaki, K. Yoshimura, K. Okada, M. Yabashi, K. Tamasaku, M. Yabashi, K. Tamasaku, A. Higashiya, T. Ishikawa, New J. Phys. **11**, 103015 (2009).
[8] K. Appavoo, D. Y. Lei, Y. Sonnefraud, B. Wang, S. T. Pantelides, S. A. Maier, R. F. Haglund, Nano Lett. **12**, 780 (2012).
[9] L. L. Fan, S. Chen, Y. F. Wu, F. H. Chen, W. S. Chu, X. Chen, C. W. Zou, Z. Y. Wu, Appl. Phys. Lett. **103**, 131914 (2013).

[10] J. Jeong, N. Aetukuri, T. Graf, T. D. Schladt, M. G. Samant, S. S. P. Parkin, Science, **339**, 1402 (2013).

[11] J. Karel, C. E. ViolBarbosa, J. Kiss, J. Jeong, N. Aetukuri, M. G. Samant, X. Kozina, E. Ikenaga, G. H. Fecher, C. Felser, S. S. P. Parkin, ACS Nano, **8**, 5784 (2014).

[12] J. R. Liang, M. J. Wu, M. Hu, J. Liu, N. W. Zhu, X. X. Xia, H. D. Chen, Chin. Phys. B, **23**, 076801 (2014).

[13] G. Andersson, Acta Chem. Scand. **10**, 623 (1956).

[14] R. M. Wentzcovitch, W. W. Schulz, P. B. Allen, Phys. Rev. Lett. **72**, 3389 (1994).

[15] V. Eyert, Ann. Phys. **11**, 650 (2002).

[16] S. Shin, S. Suga, M. Taniguchi, M. Fujisawa, H. Kanzaki, A. Fujimori, H. Daimon, Y. Ueda, K. Kosuge, S. Kachi, Phys. Rev. B, **41**, 4993 (1990).

[17] C. Weber, D. D. O'Regan, N. D. M. Hine, M. C. Payne, G. Kotliar, P. B. Littlewood, Phys. Rev. Lett. **108**, 256402 (2012).

[18] S. X. Zhang, I. S. Kim, L. J. Lauhon, Nano Lett. **11**, 1443 (2011).

[19] E. Strelcov, Y. Lilach, A. Kolmakov, Nano Lett. **9**, 2322 (2009).

[20] L. A. Sweatlock, K. Diest, Opt. Express, **20**, 8700 (2012).

[21] J. R. Liang, M. Hu, X. D. Wang, G. K. Li, A. Ji, F. H. Yang, J. Liu, N. J. Wu, H. D. Chen, Acta Phys.-Chim. Sin. **25**, 1523 (2009).

_____

[*]Corresponding author: liang_jiran@tju.edu.cn